CIRP Annals - Manufacturing Technology xxx (2018) xxx–xxx

Contents lists available at ScienceDirect

CIRP Annals - Manufacturing Technology

journal homepage: http://ees.elsevier.com/cirp/default.asp

Study of an annular laser beam based axially-fed powder cladding process

Edvard Govekar (1)[a,*], Andrej Jeromen[a], Alexander Kuznetsov[a], Gideon Levy (1)[b], Makoto Fujishima (3)[c]

[a] University of Ljubljana, Faculty of Mechanical Engineering, Ljubljana, Slovenia
[b] TTA Technology, Switzerland
[c] DMG Mori, CO., LTD., 2-35-16 Meieki, Nakamura-ku, Nagoya City, Aichi 450-0002, Japan

ARTICLE INFO

Keywords:
Additive manufacturing
Laser
Powder

ABSTRACT

An annular laser beam based powder cladding head, which enables an axial powder feeding and variation of the laser beam intensity distribution (LBID) on the workpiece surface is presented. The influence of typical LBIDs, including Ring, Tophat(−), Tophat(+), and Gaussian-like, on a cladding process has been characterized based on the process and melt pool visualization, powder catchment efficiency, clad layer geometry, and porosity. The results showed that the most stable process without plasma formation but with low dilution and porosity of the clad layer can be achieved within the range from a Ring to a Tophat (−) LBID. Additionally, axial powder feeding results in a high powder catchment efficiency above 80%.

1. Introduction

In laser metal powder cladding, the geometrical and metallurgical properties of a clad material are governed by complex laser beam – melt pool – powder stream interactions which, besides the process parameters, are also influenced by the geometrical relations of the laser beam caustic and powder stream. The latter are defined by the design of the cladding head which includes a powder nozzle, that is used to form and inject the powder stream into the melt pool created on a workpiece surface by the laser beam. Depending on the application, in commercially available cladding heads, usually a Gaussian laser beam is used, and powder is fed laterally by a single nozzle or coaxially by several discrete or a continuous nozzles [1]. The application of a Gaussian laser beam with laterally or coaxially fed powder can cause overheating at the centre of the clad, and insufficient heating at its edge. This can lead to undesirable, deep, non-uniform, and even asymmetrical dilution with a weak bond at the edge of the clad due to the higher powder density, laser beam attenuation, and higher cooling rates at the edge compared to the centre of the clad [2]. Additionally, the side and coaxial powder feeding results in a relatively low powder catchment efficiency of less than 50% [3]. In order to increase the powder catchment efficiency and to generate clads having the desired properties, the laser beam intensity and the powder density distribution should be adjusted so that a uniform heat input can be achieved over the whole width of the clad spot. For this purpose an annular laser beam cladding head, which enables axial powder feeding has been proposed [4–6].

In the paper, a novel annular laser beam (ALB) powder cladding head is presented, including a laser beam shaping unit, which, in addition to axial powder feeding, makes it possible to vary the laser beam intensity distribution (LBID) from Ring to Gaussian-like. From the presented experimental results, the advantage of axial powder feeding and the important influence of LBID on powder cladding process stability, powder catchment efficiency, and the related characteristics of the clad layer are evident. It is considered that an LBID within the range from a Ring to a Tophat is the most appropriate in the case of axially-fed fed metal powder cladding.

2. Annular laser beam — axial fed powder cladding head

The novel annular laser beam (ALB) — axial fed powder cladding head is presented schematically in Fig. 1a. It consists of a laser beam shaping unit, a guiding mirror, a laser beam focusing unit, an axial powder delivery tube and nozzle, and a coaxial shielding gas nozzle. A collimated laser beam passes through the laser beam shaping unit to be shaped into an ALB. By means of the mirror the ALB is then guided coaxially to the axis of the powder delivery tube into the focusing unit, where it is focused on the workpiece surface. In Fig. 1b some photos showing laser beam shaping and focusing units with the axial powder nozzle and the coaxial shielding gas nozzle are shown. The laser beam shaping unit can be used to shape various ALB caustics by varying the position of lens L1, which is located between the axicons A1 and A2. In Fig. 1c an example of an IR camera based measured ALB caustic with related LBID vs. the workpiece surface laser beam focal plane standoff position l_{fw} is

* Corresponding author.
E-mail address: edvard.govekar@fs.uni-lj.si (E. Govekar).

https://doi.org/10.1016/j.cirp.2018.04.082
0007-8506/© 2018 Published by Elsevier Ltd on behalf of CIRP.

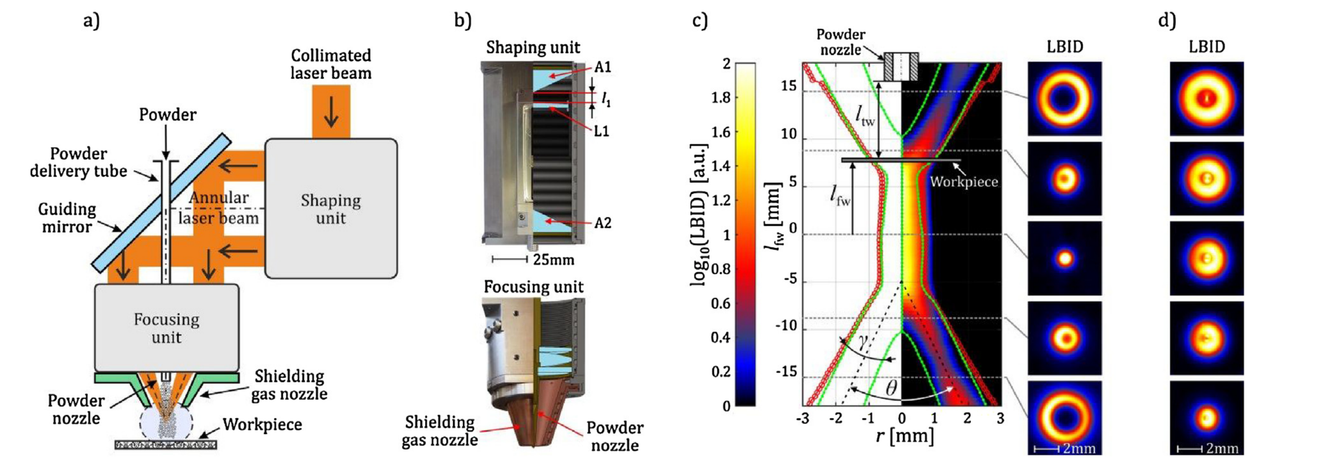

Fig. 1. (a) General arrangement of the ALB, axially-fed powder cladding head, (b) Photos of laser beam shaping and focusing units with shielding gas and axial powder nozzles, (c) Annular laser beam caustic and related LBIDs I_{lb}, (d) Example of generated LBID obtained by variation of l_1 and l_{fw}.

shown. The related convergence $\theta = 17°$ and wedge angle $\gamma = 1.5°$ of the caustic were defined based on the detection of the $1/e^2$ intensity boundaries of the LBI distribution IR images on thin metal foil, acquired at different workpiece standoff positions l_{fw}. It can be seen that by varying the position l_{fw}, the LBID and the related laser beam outer diameter d_o can be changed. Similarly the LBID can be modified by varying the position l_1 of lens L1 and of the related ALB caustic itself. By varying both positions, l_{fw} and l_1, various LBIDs can be generated, from Ring to Gaussian-like, at various outer diameters d_o. An example of a Tophat LBID with a variable outer diameter d_o is shown in Fig. 1d.

Application of the ALB enables axial feeding of the powder into the centre of the laser beam circular spot and the related melt pool generated on the workpiece surface. In the case of such feeding less laser beam attenuation, and higher powder catchment efficiency can be expected. In our case, a simple nozzle with an inner diameter $d_p = 1.0$ mm was used for this purpose. In order to characterize the powder stream at the exit from the powder nozzle, a visualization setup consisting of a vertical illumination line diode laser of wavelength 660 nm and a CMOS camera was used. The camera was positioned perpendicularly to the laser illumination plane through the axis of the powder stream. In Fig. 2a an image of the powder stream obtained by superposition of 5×10^4 images of powder particles at the exit from the powder nozzle is shown. Based on the powder particle image analysis, powder particle density distributions along the radius r were estimated at various values of the powder nozzle standoff distance l_{tw}, as shown in Fig. 2a. By calculating the related cumulative distribution $F(r)$ of the powder particles, the related powder stream radius and diameter $d_{\%}$ respectively, within which a certain % of the powder stream is contained, can be defined depending on the powder nozzle standoff distance l_{tw}, as shown in Fig. 2b. It can be seen that at a distance $l_{tw} = 8.0$ mm, the 90% powder stream diameter d_{90} is 5.6 mm.

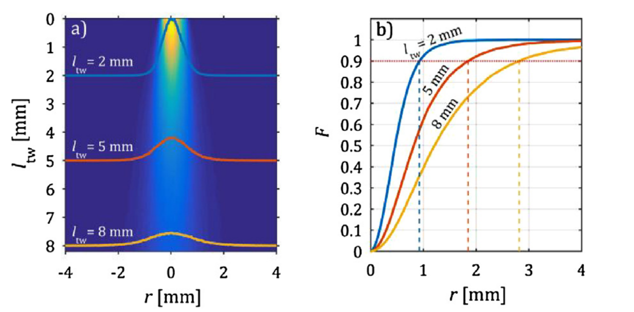

Fig. 2. (a) Powder stream with related powder particle density distribution vs. r at various positons l_{tw}, (b) related Cumulative powder density function F vs. powder stream radius r at various l_{tw}.

3. Experimental

In powder cladding experiments, the upper part ($l_{fw} > 0$ mm) of the ALB caustic was used in order to ensure shorter powder nozzle standoff distances l_{tw} and to avoid passing the powder through the high LBID region. Fig. 3a presents IR images of the four generated characteristic Ring, Tophat(−), Tophat(+), and Gaussian like LBIDs, with a four sigma diameter $d_{lb} = 3.0$ mm, which were used to investigate the influence of LBID on the axially fed powder cladding process. Using $1/e^2$ criterion, the thickness of the Ring was $d_{lb}/3$. Additionally, the instant laser beam intensity profiles I_{av} averaged along 360° and the related scanning laser beam intensity profiles I_s are shown in Fig. 3b and c. The latter are obtained by integrating the IR camera based two dimensional LBID in the feed direction and describing the accumulated energy input distribution across the feed direction.

Selected values of powder cladding parameters used in a full factorial set of $n = 32$ experiments with three repetitions are shown in Table 1. As the energy source, a CW diode laser with a wavelength range of 900–1100 nm was used. Using SS316L powder with a particle size span from 53 to 125 μm, cladding was

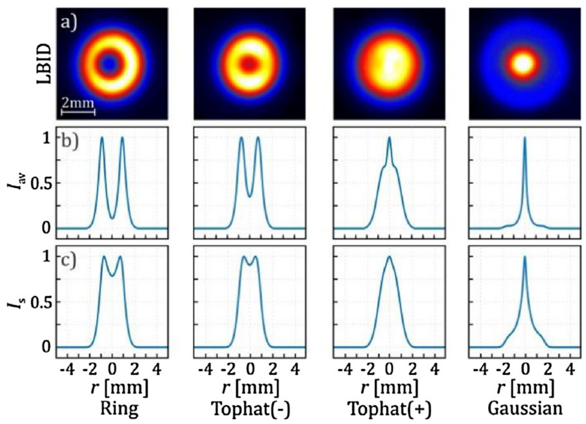

Fig. 3. (a) IR camera based images of LBID, (b) related average intensity profiles I_{av}, and (c) scanning intensity profiles I_s.

Table 1
Powder cladding process parameters.

Parameter	Value
Laser beam power – P [kW]	1.5, 2.0
Feed velocity – v_f [mm/min]	5.0, 10.0
Laser beam 4 sigma diameter – d_o [mm]	3.0
Powder mass flow – Φ_m [g/min]	8.5, 17.0
Powder carrier gas volume flow – Φ_{vp} [l/min]	0.5
Shielding gas volume flow – Φ_{vs} [l/min]	5.0
Standoff distance – l_{tw} [mm]	8.0

Please cite this article in press as: Govekar E, et al. Study of an annular laser beam based axially-fed powder cladding process. CIRP Annals - Manufacturing Technology (2018), https://doi.org/10.1016/j.cirp.2018.04.082